

Medial Septal Projections to the Parasubiculum

Inaugural-Dissertation
to obtain the academic degree
Doctor rerum naturalium (Dr. rer. nat.)

submitted to the Department of Biology, Chemistry and Pharmacy
of Freie Universität Berlin by

Daniel Parthier

27.02.2021

Contents

1	Prerequisites	5
2	Introduction	7
2.1	Theta	8
2.2	Medial Septum	9
2.3	Parasubiculum	9
2.4	Spatial Navigation	10
3	Materials and Methods	11
3.1	Animals	11
3.2	Surgical Procedures	11
3.3	<i>In-Vitro</i> Recordings	13
3.4	<i>In-Vivo</i> Recordings	15
3.5	Histological Processing	17
3.6	Acquisition and Stimulation	17
3.7	Immunohistochemistry and Histology	18
3.8	Statistical Analysis	18
4	Results	19
5	Discussion	21
	References	23
	Appendix	27
	Abbreviations	27
	Statement of contributions	28

List Of Publications	28
Eidestattliche Erklärung	28

1

Prerequisites

The experimental work of this thesis was completed from xx.xx.xx to xx.xx.xx under the supervision of Prof. Dr. Dietmar Schmitz at the Neuroscience Research Centre (NWFZ) of the Charité.

2

Introduction

The evolutionary goal of a species is to survive. This single goal is achieved by adopting to the environment and by optimising strategies to live in the specific environment and reproduce (Citation needed). Higher organisms therefore developed structures which are able to help with optimising their behaviour on different levels (citation for different evolution behaviours). One of the first developed concepts were olfaction based on chemotaxis, vision, and perception of sounds. One important higher level function, which is not solely a processing of sensory inputs, is the computation for spatial navigation (citation needed). Navigation can be observed in several species of the animal kingdom such as ants (cite), drosophila (cite), pigeons, rodents, bats, and dolphins (find citations for all) and is essential to find food, a partner, or avoiding danger. Over the last decades the endeavour to understand the “*cognitive map*” (Tolman 1948) and how we use the abstraction of space (citation needed) drove research and revealed several concepts of how space can be deconstructed (place, speed, grid, head-direction, vectors, border etc.) and represented by the brain. Coding space properties can be achieved by different mechanisms allowing for a detailed representation of the environment. If we take place cells, they can be found to fire with a higher rate in specific position which are referred to as place fields. This principle of coding properties with the count of spikes is called rate-code. However, this is not the only possible way of transferring information. An additional way a spike can code space is via the phase-code. The

phase-code is based on the fact that population activity, synaptic inputs, but also dendritic depolarisation can shape the electric field in the brain. This property is the field potential. The field potential can show oscillatory behaviour, meaning a sine-wave at specific frequencies. If one now aligns the occurrence of spikes to the phase, the position on a sine-wave, it can be observed that location can also be reflected by the phase and therefore can code additionally information via the same spike.

2.1 Theta

θ oscillations range between 4-12 Hz and were for the first time observed in the hippocampus by Green and Arduini (1954) in rabbits, cats, and monkeys. They exposed anaesthetised animals to different stimuli and measured the oscillatory responses in the hippocampal area. A decade later θ was observed in the context of navigation for the first time (Vanderwolf 1969). Freely moving rats show synchronised hippocampal activity reflected in the local field potential (LFP) during exploration (Winson 1974). Similarly these oscillations can be found in the mouse and also human, however, in humans with lower frequency (Ekstrom et al. 2005; Miller et al. 2018; Watrous et al. 2013). Interestingly enough, bat do not show a classical theta pattern during exploration (citation needed). Further, θ activity in rodents is almost constantly occurring during movement compared to burst activity in humans (Ekstrom et al. 2005; Watrous et al. 2013).

Already early on there was a consensus that oscillations are associated with navigation in behaving rodents (O’Keefe and Dostrovsky 1971; Vanderwolf 1969)

* Vanderwolf has reported (and we agree) that the former behaviours are associated with θ activity in the hippocampal EEG, while, during the latter behaviours, the EEG shows irregular slow waves.

— Footnote by J.O’Keefe & J.Dostrovsky , 1971

2.2 Medial Septum

The medial septum (MS) a structure located in the forebrain (Figure 2.1) can be found across different species.

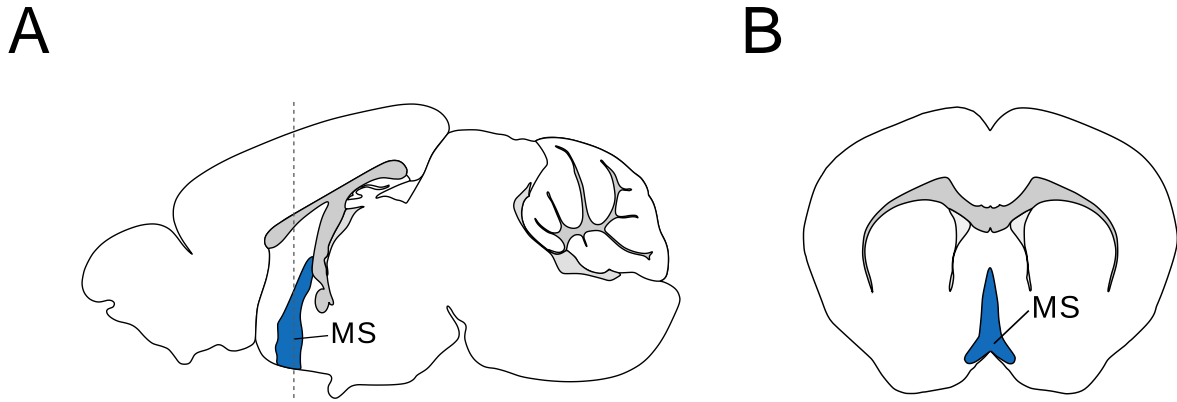


Figure 2.1: Schematic of medial septum in sagittal (A) and coronal (B) section. Blue shows the location of the MS, light gray represents ventricular space and dark gray fibre bundles. The dashed line in (A) indicates the position of the section of (B). Modified from Allen Brain Atlas.

The MS is a highly connected region and projects significantly to the hippocampus (Fuhrmann et al. 2015; Huh, Goutagny, and Williams 2010; Joshi et al. 2017; Robinson et al. 2016; Unal et al. 2018, 2015; Vandecasteele et al. 2014) and parahippocampal network (Alonso and Köhler 1984; Desikan et al. 2018; Fuchs et al. 2016; Gonzalez-Sulser et al. 2014; Groen and Wyss 1990).

2.3 Parasubiculum

The parasubiculum (PaS) on the other hand is part of the parahippocampal formation (Figure 2.2), the posterior part of the mouse brain (Boccaro et al. 2015), and is found in different species (Ding 2013). It is adjacent to the medial entorhinal cortex and presubiculum which, as the PaS, have spatially linked functional cell types coding for different aspects used for navigation (Citation needed).

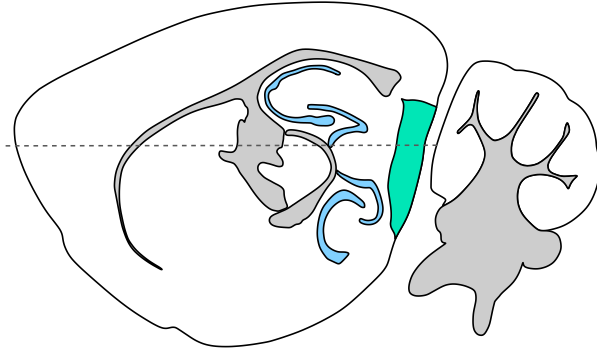
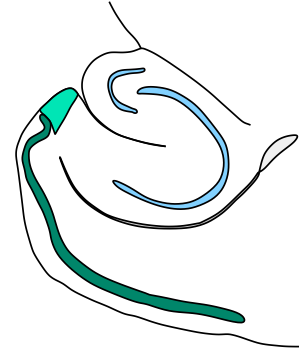
A**B**

Figure 2.2: Schematic of parasubiculum in a sagittal (A) and horizontal (B) section. turquoise shows the location of the PaS, light gray represents ventricular space and dark gray fibre bundles. The dark green in (B) represents the pyramidal cell layer II of the medial entorhinal cortex. The cornu ammonis and the dentate gyrus are marked in light blue.

2.4 Spatial Navigation

2.4.1 Theta

3

Materials and Methods

3.1 Animals

3.2 Surgical Procedures

3.2.1 Stereotactic Injections

For all surgical procedures mice were anaesthetised with isoflurane (1.5% vol/vol in oxygen, CP-Pharma Handelsgesellschaft mbH, Burgdorf, Germany) and received carprofen ($5 \frac{mg}{kg}$) as analgesia additionally to subcutaneous application of lidocaine as local analgesia at the side of incision. Animals were placed into a stereotaxic frame where they were fixed and stabilised with ear bars. After disinfecting the place of incision with iodide (##### find exact one####) an one cm incision was performed on the midline. The skin was pushed and fixed to the side so that the skull was easily accessible.

The skull was virtually levelled using a robot stereotaxic (Neurostar, Tübingen, Germany) and a craniotomy drilled at the position of entry (in mm from bregma: 0.7 anteriorposterior, 0.7 mediolateral). A NanoFil syringe (World Precision Instruments, LCC., Sarasota County, FL, US) with a 34-gauge needle with adeno-associated virus 1 (AAV1) containing the plasmid for the yellow fluorescent protein (YFP) and chan-

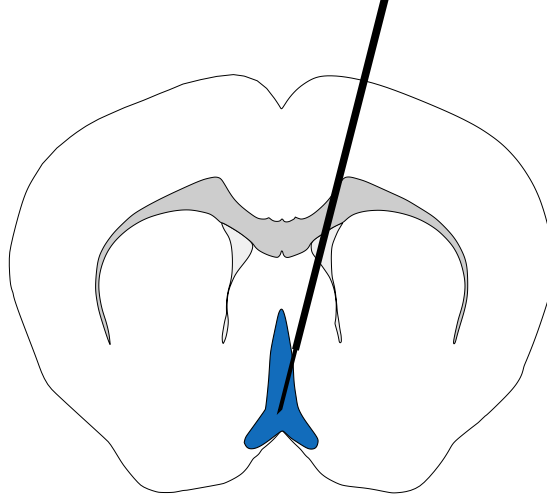


Figure 3.1: Schematic of medial septum (blue) and the injection canula (black). A 10° angle is used to avoid damage to superior sagittal sinus which is located on the midline on top of the brain surface (not shown).

nelrhodopsin (*pAAV-EF1 α -doublefloxed-hChR2(H134R)-EYFP-WPR* at $6.26 \cdot 10^{11}$ VG/ml) was placed with a 10° angle through the hole and slowly moved 3.8 mm downwards along the dorsoventral axis to the MS (Figure 3.1). The position was held for 5 min before 200 nl of the virus was injected at a rate of 40 nl/min. The needle was left for further 5 min until it was slowly withdrawn. During the whole procedure the animal's temperature was maintained at 37°C , eyes were covered with eye-cream to provide moisture, and anaesthesia was checked regularly. The incision was closed and the animal was put back to the home-cage to recover where it woke up after less than 15 min. Animals were checked daily and were allowed to recover for at least 4 weeks.

3.2.2 Headbar Implant

Previously injected animals as part of *in-vivo* awake head-fixed recordings were given a headbar implant. Surgical procedures were similar to 3.2.1, however, after the incision a craniotomy was made at a more anterolateral position (in mm from bregma: 1.2 anteriorposterior, 1.2 mediolateral) to place a screw for grounding. The screw was fixed without damaging the surface of the brain. The skull surface was then sealed using OptiBond™ Solo Plus (KerrHawe SA, Bioggio, Switzerland) and the golden pin

attached to the screw was stabilised using CHARISMA® ABC A1 (Kulzer GmbH, Hanau, Germany). A headbar was placed over the skull, aligned to midline and fixed with Paladur® dental cement (Kulzer GmbH, Hanau, Germany). The animal was then released back to the home-cage where it could recover for at least 2 days before habituation began.

3.3 *In-Vitro* Recordings

3.3.1 Slice Preparation

For slices animals (n = XX PV-Cre mice, n = XX ChAT-Cre mice) were deeply anaesthetised under isoflurane and then decapitated. The brain was quickly removed and transferred to ice-cold ($\sim 4^{\circ}\text{C}$) slicing solution (sucrose artificial cerebral spinal fluid – sACSF). sACSF contained (mM): 87 NaCl, 26 NaHCO₃, 10 Glucose, 50 Sucrose, 2.5 KCl, 1.25 NaH₂PO₄, 0.5 CaCl₂, 3 MgCl₂ · 6H₂O. The forebrain was separated from the rest by making a coronal cut. The posterior part of the brain was separated with a sagittal cut in the two hemispheres. The two posterior Hemispheres and the forebrain were placed on a vibrating blade microtome (VT1200S, Leica Biosystems, Wetzlar, Germany) to produce 400 μm horizontal and coronal slices (Figure 2.2 B) which were then transferred to an interface chamber for up to 1-6 h storage. Slices were superfused constantly with oxygenated ACSF (in mM: 119 NaCl, 26 NaHCO₃, 10 Glucose, 2.5 KCl, 1 NaH₂PO₄, 2.5 CaCl₂, 1.3 MgCl₂ · 6H₂O). All solutions were saturated in oxygen using carbogen (95% O₂ and 5% CO₂). To verify channelrhodopsin expression fluorescence was checked in medial septal coronal sections under a fluorescence microscope (DM3000, Leica Biosystems, Wetzlar, Germany) prior to recordings.

3.3.2 Slice Recordings

Slices were transferred from the interface storage to the recording chamber where they were constantly superfused (at 3.5 ml/min) with oxygenated ACSF and maintained at

32-34°C. Cells were visually identified using an upright microscope (BX51W1, Olympus, Tokyo, Japan) and infrared differential interference contrast microscopy through a digital camera (XM10-IR, Olympus, Tokyo, Japan). To record in the whole-cell patch-clamp configuration a borosilicate glass electrode (Harvard Apparatus, Holliston, Massachusetts, USA) was pulled on a DMZ-Universal-Electrode-Puller (Zeitz-Instruments, Martinsried, Germany) to 2.5-6 M Ω and filled with intracellular solution (in mM: 120 K-Gluconate, 10 HEPES, 10 KCl, 5 EGTA, 2 MgSO₄ · 7H₂O, 3 MgATP, 1 NaGTP, 5 Phosphocreatine Na, 0.2% Biocytin). Data was recorded with a Multiclamp 700A/B (Molecular Devices, LLC., San Jose, CA, USA) where signals were filtered at 10 kHz, sampled at 20 kHz and then digitised. Data was either digitised by a Digidata 1550 (Molecular Devices, LLC., San Jose, CA, USA) for use in pClamp. In recordings in IGB Pro 6.12 (WaveMetrics, Inc., Portland, OR, USA) or WinWCP V5.3.7 (Dempster 1997) a BNC-2090 interface board (PCI 6035E A/D Board, National Instruments, Austin, Texas, USA) or a USB-6229 BNC (National Instruments, Austin, Texas, USA) was used for digitisation. After opening, cells were held in voltage-clamp at -60 mV to measure series resistance and assess access. Cells were then switched to current-clamp configuration to perform a characterisation of somatic properties (current steps of 40-100 pA). To assess septal connectivity to the parasubiculum channelrhodopsin expressing fibres in the area were activated by 10 ms light pulses from a LED (CoolLED pE-2, Andover, UK) or an halogen lamp (### check for model ####) coupled to the 60x objective. To elicit inhibitory (IPSPs) or excitatory postsynaptic potentials (EPSPs) and inhibitory (IPSCs) or excitatory postsynaptic currents (EPSCs) a range of light pulse frequencies (10, 20, 40 Hz) was used. Additionally, inputs hidden due to low driving force or simultaneously occurring synaptic inputs were unmasked by changing the holding potential of the cell from -60, to -80 and then to -50 mV after at least 10 trials respectively. In some recordings (##### N number #####) monosynaptic inputs were validated by at first blocking with 1 μ M tetrodotoxin (TTX) and then reinstating inputs by depolarising the terminals with ## μ M## 4-Aminopyridine (4-AP). Liquid junction potential was not corrected for. Slices were fixed in 4% paraformaldehyde (PFA) overnight for immunohistochemistry stainings.

Drugs used: 4-Aminopyridine (Tocris Bioscience, Bristol, UK) NBQX disodium salt (Tocris Bioscience, Bristol, UK) SR 95531 hydrobromide (Tocris Bioscience, Bristol, UK)

3.4 *In-Vivo* Recordings

3.4.1 Anaesthetised Recordings

Before recordings the animals was anaesthetised as described under 3.2.1. A craniotomy was performed at 1 anteroposterior and 1 mediolateral (in mm from bregma) and two additional ones at ± 2.5 mediolateral and 0 ##### anteroposterior (in mm from lamda). The animal was injected with ### $\frac{mg}{kg}$ urethane and subsequently transferred to the recording setup where two ISO-3x-tet-lin optrodes (NeuroNexus, Ann Arbor, MI, USA) with 32 channels each were used to record in the MS and PaS simultaneously and allowed for light stimulation of both regions. The probe targeting the medial septum was placed with an angle of 10° and lowered 4.3 mm from the surface. The optrode targeting the PaS was lowered perpendicular to the brains surface with 2.5-35 mm distance from the surface.

3.4.2 Head-Fixed Awake Immobile Recordings

For head-fixed recordings in immobile mice animals were habituated to the setup and trained to stand still in a paper roll whilst being fixed at the headbar. Animals were trained for 5-7 days with increasing time duration until they were able to remain still for up to an hour. After training sessions mice were rewarded with condense milk. After the training period animals were anaesthetised as described in 3.2.1. A craniotomy was performed at 1 anteroposterior and 1 mediolateral (in mm from bregma) and another craniotomy at -2.5 mediolateral and 0 ##### anteroposterior (in mm from lamda). The probe targeting the medial septum was placed with an angle of 10° and lowered 4.3 mm from the surface. The optrode targeting the PaS was lowered

perpendicular to the brains surface with 2.5-35 mm distance from the surface. After the recording session Kwik-Cast (World Precision Instruments Ltd, Hertfordshire, UK) was applied to the craniotomies to protect the brain from drying out.

3.4.3 Head-Fixed Awake Recordings on Treadmill

For head-fixed recordings on the treadmill animals were water deprived to encourage them to drink during the training sessions. During the training sessions animals were trained to run on the treadmill whilst being fixed at the headbar.

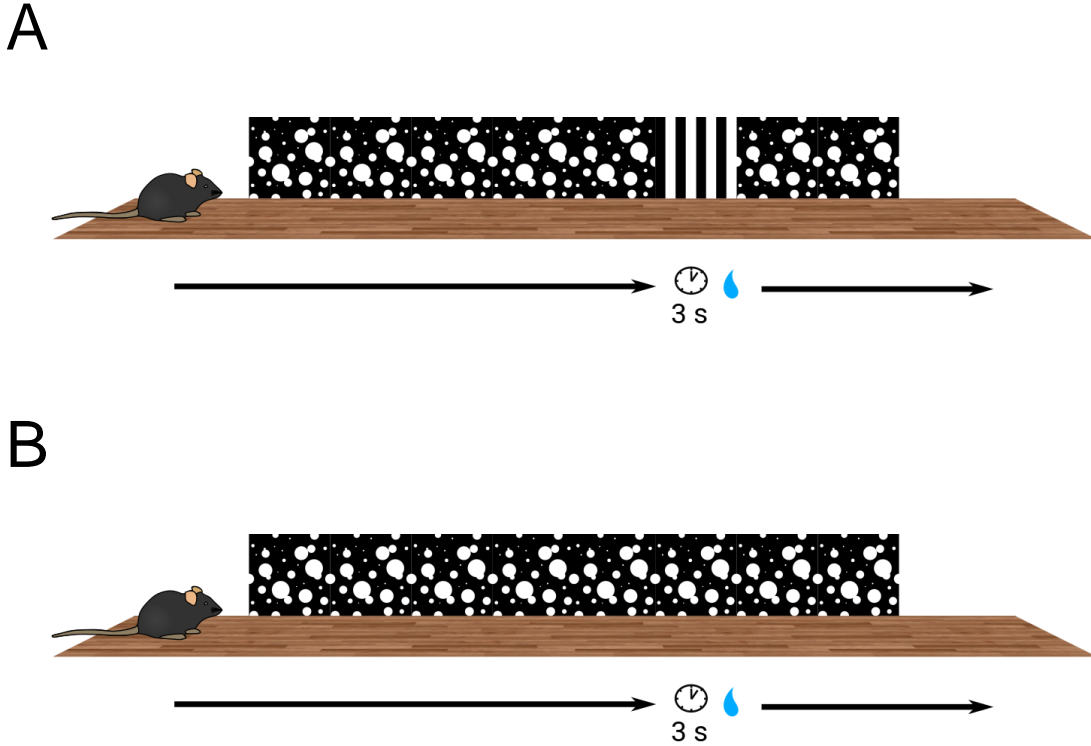


Figure 3.2: Schematic of linear track. In A the wall of the reward zone (120-140 cm) is striped so that it can be distinguished by the mouse from the rest of the environment. The animal had to reach the reward zone, wait for 3 s and then got a water reward. B represents the same task but without the beaconed reward zone.

The virtual reality (VR) task entailed a linear track which was 200 cm long and had a reward zone at 120 cm to 140 cm (Figure 3.2). The animal firstly, had to reach the reward zone and spent a fixed amount of time (3 s) until a water reward was delivered via a pump. Subsequently, the animal had to reach the end of the track where it was

then teleported back to the start. After a waiting period of 5 s a new trial began. Animals were trained for 3 weeks with increasing time duration until they were able to run and perform a distance estimation task. For the recording session animals were surgically prepared as described in 3.4.2 and placed on the treadmill to perform the task. Light stimulation was used for a whole trial after a minimum of 5 trials. At the end of the trial light was switched back off and the animal continued with the trials. This alternating procedure was repeated for the whole recording session in order to gather multiple trials during stimulation. During training sessions four beacons trials (Figure 3.2A) were followed by an non-beacons trial (Figure 3.2B) which had no distinguishable reward zone. For Recording sessions the frequency was increased to 2 beacons trials followed by a non-beacons trial.

3.5 Histological Processing

Animals from *in-vivo* recordings were perfused after the final recording session. Therefore, they were deeply anaesthetised using urethane ($2.5 \frac{g}{kg}$ body weight) and transcardially perfused with phosphate-buffered saline (PBS) followed by 4% PFA. The fixed brain was removed and stored in 4% PFA over night. After post-fixation brains were washed in PBS before being they were dissected into two hemispheres and a forebrain part. The three parts were blocked onto a vibrating blade microtome (Leica VT1000S, Leica Biosystems, Wetzlar, Germany) and sliced into 75 μm thick sagittal (hemispheres containing the PaS) and coronal (forebrain containing the MS) sections.

3.6 Acquisition and Stimulation

Signals were acquired and digitised using a RHD2000 system (Intan Technologies, Los Angeles, CA, USA). The light stimulation was performed using Spike2 coupled to an Power1401-3A data acquisition interface (Cambridge Electronic Design Limited, Cambridge, UK). Custom scripts were used to drive pulse and sine wave stimulations at

different frequencies (1 Hz, 2 Hz, 4 Hz, 8 Hz, 16 Hz, 32 Hz). 1 Hz (2 ms pulse length) stimulation was used to identify channelrhodopsin expressing cells in the MS whereas higher frequencies were used to drive network activity in the MS and the PaS. For pulse stimulations between 2 and 8 Hz nested pulse bursts (5 times 5 ms single pulse) were used to imitate theta burst activity. Pulse frequencies at 16 and 32 Hz were achieved through single 10 ms long pulses.

3.7 Immunohistochemistry and Histology

Anti-NeuN purified Antibody (ABN90P, Sigma-Aldrich, St. Louis, MO, United States, Sigma-Aldrich, St. Louis, Missouri, United States) Anti-Reelin Antibody (MAB5364) WFS1 Polyclonal antibody - Rabbit/IgG (11558-1-AP, Proteintech Group, Inc, Rosemont, IL, USA)

3.8 Statistical Analysis

4

Results

Here is a review of existing methods.

5

Discussion

Here is a review of existing methods.

References

- Alonso, Angel, and Christer Köhler. 1984. “A Study of the Reciprocal Connections Between the Septum and the Entorhinal Area Using Anterograde and Retrograde Axonal Transport Methods in the Rat Brain.” *Journal of Comparative Neurology* 225 (3): 327–43. <https://doi.org/https://doi.org/10.1002/cne.902250303>.
- Boccaro, Charlotte N, Lisa J Kjonigsen, Ingvild M Hammer, Jan G Bjaalie, Trygve B Leergaard, and Menno P Witter. 2015. “A Three-plane Architectonic Atlas of the Rat Hippocampal Region.” *Hippocampus* 25 (7): 838–57. <https://doi.org/10.1002/hipo.22407>.
- Dempster, J. 1997. “A New Version of the Strathclyde Electrophysiology Software Package Running Within the Microsoft Windows Environment.” *Journal of Physiology* 504 (Suppl.): P57–P57.
- Desikan, Srinidhi, David E Koser, Angela Neitz, and Hannah Monyer. 2018. “Target Selectivity of Septal Cholinergic Neurons in the Medial and Lateral Entorhinal Cortex.” *Proc. Natl. Acad. Sci. U.S.A.* 115 (11): E2644–E2652. <https://doi.org/10.1073/pnas.1716531115>.
- Ding, Song-Lin L. 2013. “Comparative Anatomy of the Prosubiculum, Subiculum, Presubiculum, Postsubiculum, and Parasubiculum in Human, Monkey, and Rodent.” 521 (18): 4145–62. <https://doi.org/10.1002/cne.23416>.
- Ekstrom, Arne D., Jeremy B. Caplan, Emily Ho, Kirk Shattuck, Itzhak Fried, and Michael J. Kahana. 2005. “Human Hippocampal Theta Activity During Virtual Navigation.” *Hippocampus* 15 (7): 881–89. <https://doi.org/10.1002/hipo.20109>.

- Fuchs, Elke C, Angela Neitz, Roberta Pinna, Sarah Melzer, Antonio Caputi, and Hannah Monyer. 2016. “Local and Distant Input Controlling Excitation in Layer II of the Medial Entorhinal Cortex.” *Neuron* 89 (1): 194–208. <https://doi.org/10.1016/j.neuron.2015.11.029>.
- Fuhrmann, Falko, Daniel Justus, Liudmila Sosulina, Hiroshi Kaneko, Tatjana Beutel, Detlef Friedrichs, Susanne Schoch, Martin K Schwarz, Martin Fuhrmann, and Stefan Remy. 2015. “Locomotion, Theta Oscillations, and the Speed-Related Firing of Hippocampal Neurons Are Controlled by a Medial Septal Glutamatergic Circuit.” *Neuron* 86 (5): 1253–64. <https://doi.org/10.1016/j.neuron.2015.05.001>.
- Gonzalez-Sulser, Alfredo, Daniel Parthier, Antonio Candela, Christina McClure, Hugh Pastoll, Derek Garden, Gülşen Sürmeli, and Matthew F Nolan. 2014. “GABAergic Projections from the Medial Septum Selectively Inhibit Interneurons in the Medial Entorhinal Cortex.” *J. Neurosci.* 34 (50): 16739–43. <https://doi.org/10.1523/JNEUROSCI.1612-14.2014>.
- Green, John D., and Arnaldo A. Arduini. 1954. “HIPPOCAMPAL ELECTRICAL ACTIVITY IN AROUSAL.” *Journal of Neurophysiology* 17 (6): 533–57. <https://doi.org/10.1152/jn.1954.17.6.533>.
- Groen, T van, and JM Wyss. 1990. “The Connections of Presubiculum and Parasubiculum in the Rat.” *Brain Res.* 518 (1-2): 227–43.
- Huh, C Y L, R Goutagny, and S Williams. 2010. “Glutamatergic Neurons of the Mouse Medial Septum and Diagonal Band of Broca Synaptically Drive Hippocampal Pyramidal Cells: Relevance for Hippocampal Theta Rhythm.” *The Journal of Neuroscience* 30 (47): 15951–61. <https://doi.org/10.1523/jneurosci.3663-10.2010>.
- Joshi, Abhilasha, Minas Salib, Tim J Viney, David Dupret, and Peter Somogyi. 2017. “Behavior-Dependent Activity and Synaptic Organization of Septo-Hippocampal GABAergic Neurons Selectively Targeting the Hippocampal CA3 Area.” *Neuron* 96 (6): 1342–1357.e5. <https://doi.org/10.1016/j.neuron.2017.10.033>.

- Miller, Jonathan, Andrew J. Watrous, Melina Tsitsiklis, Sang Ah Lee, Sameer A. Sheth, Catherine A. Schevon, Elliot H. Smith, et al. 2018. “Lateralized Hippocampal Oscillations Underlie Distinct Aspects of Human Spatial Memory and Navigation.” *Nature Communications* 9 (1): 2423. <https://doi.org/10.1038/s41467-018-04847-9>.
- O’Keefe, J., and J. Dostrovsky. 1971. “The Hippocampus as a Spatial Map. Preliminary Evidence from Unit Activity in the Freely-Moving Rat.” *Brain Research* 34 (1): 171–75. [https://doi.org/10.1016/0006-8993\(71\)90358-1](https://doi.org/10.1016/0006-8993(71)90358-1).
- Robinson, Jennifer, Frédéric Manseau, Guillaume Ducharme, Bénédicte Amilhon, Erika Vigneault, Salah El Mestikawy, and Sylvain Williams. 2016. “Optogenetic Activation of Septal Glutamatergic Neurons Drive Hippocampal Theta Rhythms.” *J. Neurosci.* 36 (10): 3016–23. <https://doi.org/10.1523/JNEUROSCI.2141-15.2016>.
- Tolman, Edward C. 1948. “Cognitive Maps in Rats and Men.” *Psychological Review* 55 (4): 189–208. <https://doi.org/10.1037/h0061626>.
- Unal, Gunes, Michael G Crump, Tim J Viney, Tímea Éltés, Linda Katona, Thomas Klausberger, and Peter Somogyi. 2018. “Spatio-Temporal Specialization of GABAergic Septo-Hippocampal Neurons for Rhythmic Network Activity.” *Brain Struct Funct*, 1–24. <https://doi.org/10.1007/s00429-018-1626-0>.
- Unal, Gunes, Abhilasha Joshi, Tim J Viney, Viktor Kis, and Peter Somogyi. 2015. “Synaptic Targets of Medial Septal Projections in the Hippocampus and Extrahippocampal Cortices of the Mouse.” *J. Neurosci.* 35 (48): 15812–26. <https://doi.org/10.1523/JNEUROSCI.2639-15.2015>.
- Vandecasteele, Marie, Viktor Varga, Antal Berényi, Edit Papp, Péter Barthó, Laurent Venance, Tamás F F Freund, and György Buzsáki. 2014. “Optogenetic Activation of Septal Cholinergic Neurons Suppresses Sharp Wave Ripples and Enhances Theta Oscillations in the Hippocampus.” *Proc. Natl. Acad. Sci. U.S.A.* 111 (37): 13535–40. <https://doi.org/10.1073/pnas.1411233111>.
- Vanderwolf, C. H. 1969. “Hippocampal Electrical Activity and Voluntary Movement in the Rat.” *Electroencephalography and Clinical Neurophysiology* 26 (4): 407–18.

[https://doi.org/10.1016/0013-4694\(69\)90092-3](https://doi.org/10.1016/0013-4694(69)90092-3).

- Watrous, Andrew J., Darrin J. Lee, Ali Izadi, Gene G. Gurkoff, Kiarash Shahlaie, and Arne D. Ekstrom. 2013. “A Comparative Study of Human and Rat Hippocampal Low-Frequency Oscillations During Spatial Navigation: Comparison of Human and Rodent Theta.” *Hippocampus* 23 (8): 656–61. <https://doi.org/10.1002/hipo.22124>.
- Winson, Jonathan. 1974. “Patterns of Hippocampal Theta Rhythm in the Freely Moving Rat.” *Electroencephalography and Clinical Neurophysiology* 36 (January): 291–301. [https://doi.org/10.1016/0013-4694\(74\)90171-0](https://doi.org/10.1016/0013-4694(74)90171-0).

Appendix

Abbreviations

Table 5.1: List of Abbreviations

4-AP	4-Aminopyridine
ACSF	Artificial Cerebral Spinal Fluid
ChAT	Choline Acetyltransferase
EPSC	Excitatory Postsynaptic Current
EPSP	Excitatory Postsynaptic Potential
IPSC	Inhibitory Postsynaptic Current
IPSP	Inhibitory Postsynaptic Potential
LFP	Local Field Potential
LS	Lateral Septum
MEC	Medial Entorhinal Cortex
MS	Medial Septum
PBS	Phosphate-Buffered Saline
PFA	Paraformaldehyde
PV	Parvalbumin
PaS	Parasubiculum
PrS	Presubiculum
TTX	Tetrodotoxin
VR	Virtual Reality

Table 5.1: List of Abbreviations

sACSF	Sucrose Artificial Cerebral Spinal Fluid
-------	--

Statement of contributions

List Of Publications

Eidestattliche Erklärung

Hiermit versichere ich,

Daniel Parthier (Matrikelnummer: 5144911) geboren am 05.08.1987 in Potsdam, an Eides statt, dass die vorliegende Arbeit von mir selbstständig und ohne unerlaubte Hilfe Dritter verfasst wurde und ich keine anderen als die angegebenen Quellen und Hilfsmittel verwendet sowie wörtliche und sinngemäße Zitate als solche kenntlich gemacht habe. Diese Arbeit hat in gleicher oder ähnlicher Form noch keiner anderen Prüfungsbehörde vorgelegen und wurde bisher nicht veröffentlicht.

Berlin, 27.02.2021 Unterschrift